Fluid Phase Equilibria 388 (2015) 100–106

Contents lists available at ScienceDirect

Fluid Phase Equilibria

journal homepage: www.elsevier.com/locate/fluid

Carbon dioxide solubility in aqueous solutions of NaCl: Measurements and modeling with electrolyte equations of state

Pedro J. Carvalho [a,*], Luís M.C. Pereira [a], Neusa P.F. Gonçalves [a], António J. Queimada [b], João A.P. Coutinho [a,**]

[a] CICECO, Departamento de Química, Universidade de Aveiro, 3810-193 Aveiro, Portugal
[b] INFOCHEM, KBC Process Technology, Unit 4, The Flag Store, 23 Queen Elizabeth Street, SE1 2LP London, UK

ARTICLE INFO

Article history:
Received 13 June 2014
Received in revised form 16 December 2014
Accepted 29 December 2014
Available online 30 December 2014

Keywords:
Carbon dioxide
Water
NaCl
Henry's constant
CPA-Infochem EoS
RKSA-Infochem EoS
Electrolytes

ABSTRACT

A new high pressure cell was developed to measure the high pressure phase behavior of gas + aqueous salt solutions and validated through the measurement, and comparison against literature data, of two systems, the $H_2O + CO_2$ and $H_2O + CO_2 + NaCl$, at temperatures up to 363 K and pressures up to 13 MPa. As previously reported by others, a *salting out* effect on the carbon dioxide solubility in water by NaCl is observed, decreasing its solubility as the salt concentration increases. Electrolyte versions of the cubic-plus-association and the RKSA-Infochem equations of state were used to estimate the $H_2O + CO_2$ and $H_2O + CO_2 + NaCl$ phase behavior, with both EoS providing a good representation of the experimental data.

1. Introduction

Carbon capture and storage (CCS) technologies are expected to play a key role in strategies to mitigate climate changes, by ensuring large reductions in the rising CO_2 emissions from the continued use of fossil fuels. Although the technologies for CCS are being successfully developed, often in a "learning by doing" basis [1], with some ready for demonstration, several concerns and challenges are still present [1–3]. Key areas like methodologies to identify and assess safe underground storage sites and their monitoring, during and after CO_2 injection, or the risks to health, ecosystems and atmosphere due to CO_2 leakages are still poorly known and highly relevant. Furthermore, storing CO_2 deep below the earth's surface or saline aquifers stands as one of the most promising approaches and the knowledge of the CO_2 behavior in the surrounding environment stands as highly relevant to the proper long-term environmental safe storage.

Carbon dioxide enhanced oil recovery (CO_2-EOR) has been branded as the next generation of oil production and has been gaining enormous interest within oil companies, as an ecological, technical, economical and profitable technique to attain value to undervalued or once considered depleted fields. Water alternating gas (wag) method alternates the injection of CO_2 with water/brine and stands as one of the most promising methods to CO_2-EOR [4,5].

The knowledge of the CO_2 behavior in water and in aqueous salt solutions is thus of key importance. In this work, a new apparatus was developed to investigate the high pressure phase behavior of gas + water and gas + aqueous salt solutions. Two systems, the $H_2O + CO_2$ and $H_2O + CO_2 + NaCl$ were investigated, at temperatures up to 363 K and pressures up to 13 MPa, and both the equipment and methodology were validated through comparison with literature data. The gas–liquid equilibrium data for the $CO_2 + H_2O$ and $CO_2 + H_2O + NaCl$ systems were selected due to the large set of high quality experimental data, widely available in literature, that covers a large range of pressures, temperatures, CO_2 compositions and salt molalities.

Electrolyte versions of the cubic-plus-association (CPA) and the RKSA-Infochem equations of state (EoS) were used to estimate the experimental data measured in this work and that available in the literature. It will be shown that both EoS provide a good representation of the experimental data with the RKSA-Infochem + electrolyte EoS slightly out-performing the CPA-Infochem + electrolyte EoS.

* Corresponding author. Tel.: +351 234 370 958; fax: +351 234 370 084.
** Corresponding author. Tel.: +351 234 401 507; fax: +351 234 370 084.
E-mail addresses: quijorge@ua.pt (P.J. Carvalho), jcoutinho@ua.pt (J.A.P. Coutinho).

http://dx.doi.org/10.1016/j.fluid.2014.12.043
0378-3812/

Table 1
Bubble point data of the system $CO_2 + H_2O$.

x_{CO_2}	T/K	p/MPa	x_{CO_2}	T/K	p/MPa	x_{CO_2}	T/K	p/MPa	x_{CO_2}	T/K	p/MPa
0.003	293.18	0.31	0.006	293.33	0.81	0.008	293.17	1.31	0.010	293.29	1.63
	303.28	0.52		303.54	1.19		303.24	1.80		303.87	2.30
	313.17	0.67		313.58	1.58		313.40	2.25		313.87	2.79
	323.15	0.90		323.39	1.96		323.52	2.80		322.97	3.50
	332.88	1.14		333.74	2.31		333.39	3.25		333.62	4.00
	343.25	1.31		343.17	2.60		343.12	3.80		343.65	4.80
	353.42	1.49		353.17	3.01		353.48	4.35		352.99	5.31
	363.04	1.71		363.15	3.27		363.42	4.78		362.98	5.87
0.012	283.55	1.29	0.015	283.41	1.73	0.018	283.24	2.02	0.020	283.35	2.36
	293.13	1.94		293.13	2.51		293.48	2.98		293.27	3.43
	303.20	2.68		303.28	3.35		303.08	4.08		303.42	4.87
	313.16	3.30		313.19	4.32		313.30	5.48		313.37	6.53
	323.19	4.10		322.94	5.25		323.17	6.85		323.24	8.37
	333.12	4.80		333.19	6.41		333.20	8.27		333.06	10.34
	343.06	5.71		343.29	7.50		343.18	9.68		342.96	11.99
	353.00	6.37		353.31	8.49		352.91	11.03			
	363.19	6.95		363.11	9.54		363.12	12.08			

Standard uncertainties u are $u(T) = 0.15$ K, $u(x) = 0.0002$ and $u(p) = 0.004$ MPa.

2. Experimental

2.1. Chemicals

The water used was double distilled, passed by a reverse osmosis system, and further treated with a Milli-Q Plus 185 water purification apparatus. It has a resistivity of 18.2 MΩ cm, a total organic content (TOC) smaller than 5 μg L^{-1}, and it is free of particles greater than 0.22 μm. The NaCl used was acquired from AnalaR Normapur with a purity of ≥99.9%.

The CO_2 used was acquired from Air Liquide with a purity of ≥99.998% and H_2O, O_2, C_nH_m, N_2 and H_2 impurities volume fractions lower than $(3, 2, 2, 8 \text{ and } 0.5) \times 10^{-6}$, respectively.

2.2. Solubility measurements

The high pressure equilibrium cell used in this work is based on a cell designed by Daridon and co-workers [6–9] using the synthetic method and can operate up to 70 MPa and in the (283–373) K temperature range. The high pressure equilibrium cell is made of a hastelloy C276 alloy league highly resistant to corrosion and identical to other cell, available in our laboratory, that was described in previous works and whose methodology shown to be adequate to accurately measure gas–liquid equilibria in a wide range of fluids, including alkanes and ionic liquids and their aqueous solutions, at variable pressures and temperatures [10–17].

The high pressure equilibrium cell consists of a horizontal hollow hastelloy C276 alloy cylinder, closed at one end by a movable piston and at the other end by a sapphire window, from which the operator follows the behavior of the sample with pressure (up to 70 MPa) and in the (293–363) K temperature range. The cell is thermostatized by circulating a heat-carrier fluid, thermo regulated using a thermostat bath circulator (Jubalo MC F25) with a temperature stability of 0.01 K, through three flow lines directly connected to the cell. The temperature inside the cell is measured by a high precision Pt100 thermometer, with an uncertainty of 0.15 K, inserted in the cell, close to the sample. The pressure is measured by a piezoresistive silicon pressure transducer (Kulite HEM 375) fixed directly inside the cell to reduce dead volumes, which was previously calibrated and certified by an independent laboratory with IPAC accreditation, following the EN 837-1 standard and with accuracy better than 0.2%. The homogenization of the mixture is held by a small magnetic bar placed inside the cell and an external magnetic stirrer.

According to the applied synthetic method, a fixed amount of water, whose exact mass is determined by weight using a high weight/high precision balance (Sartorius LA2000P) with an accuracy of 1 mg, is introduced into the cell, that is under vacuum, though means of a flexible pressure capillary. The water used was previously degassed by means of an ultra-sonic bath, for 30 min, before its transfer into the cell. For the systems containing salts the methodology is similar: the salt is mixed in the water and the mixture of known composition is transferred into the cell as

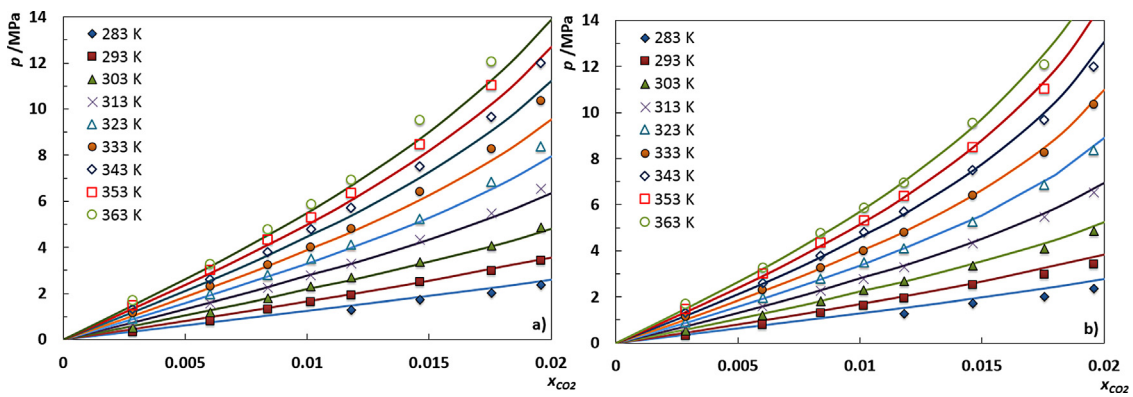

Fig. 1. Pressure–composition diagram of the binary system $CO_2 + H_2O$. The lines represent the CPA-Infochem + electrolyte EoS (a), the RKSA-Infochem + electrolyte EoS (b).

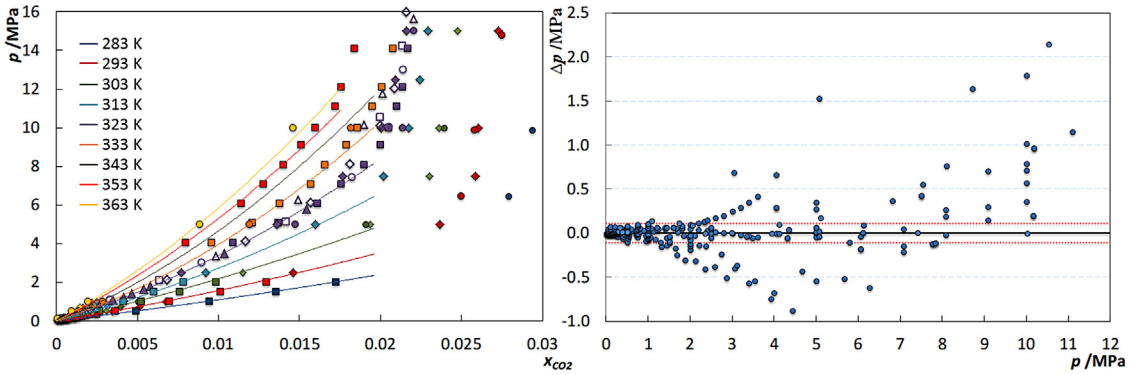

Fig. 2. Pressure–composition diagram of the binary system $CO_2 + H_2O$ (left) with lines representing the experimental data and the symbols the literature data, and pressure deviation between experimental and literature data [33–53] as a function of pressure (right). The red dotted lines represent the absolute average deviations obtained. (For interpretation of the references to color in this figure legend, the reader is referred to the web version of this article.)

described before. The gas is introduced under pressure, from an ultra-lightweight composite cylinder, by means of a flexible pressure capillary and its mass measured with a high weight/high precision balance.

Once the mixture with known compositions is prepared inside the cell and the desired temperature at low pressure is reached, the pressure is then slowly increased until the system becomes monophasic. The pressure at which the last bubble disappears, for that fixed temperature and composition, represents the equilibrium pressure.

3. Modeling

For modeling aqueous electrolyte solutions we need to add an electrolyte term to our thermodynamic model. Using cubic equations of state, such as the Soave–Redlich–Kwong (SRK), the residual Helmholtz energy function needs to be expanded into different contributions: a cubic contribution (A^r_{cubic}) to account for van der Waals interactions, an association contribution (A^r_{assoc}) based on a simplified version of the association theory developed by Wertheim [18,19] to account for hydrogen bonding and stronger solvation effects and an electrolyte contribution ($A^r_{electrolyte}$) that represents the effect of dissolved salts on mixed solvents, based on the Debye–Hückel theory.

$$A^r = A^r_{cubic} + A^r_{assoc} + A^r_{electrolyte} \quad (1)$$

Further details on the different contributions used here are presented elsewhere [20].

In this work the Multiflash™ 4.4 package was used to estimate CO_2 solubilities in both pure water and NaCl solutions of different molalities as a function of temperature and pressure. Two equations of state are available in Multiflash™ 4.4 for that purpose: CPA-Infochem + electrolyte and RKSA-Infochem + electrolyte. The difference between the two electrolyte equations of state are related to the incorporation (or not) of the association contribution and to how the mixture energy parameter (a), in the cubic term, is determined. While CPA-Infochem + electrolyte includes the association contribution in Eq. (1) and determines the mixture energy parameter using a van der Waals 1-fluid mixing rule, the RKSA-Infochem + electrolyte model uses an excess Gibbs energy mixing rule for the mixture energy parameter, but does not include an explicit association contribution.

The CPA EoS has been extensively used in the literature to model different associating systems and showed to be able to provide the correct description of the water solubility in hydrocarbons [21–24], fatty acid esters and biodiesels [25], the atmospheric [26] and near/supercritical [27] vapor–liquid–equilibria of fatty acid ester + alcohol systems, and the liquid–liquid equilibria of multi-component systems containing hydrocarbons, fatty acid esters, alcohols, glycerol, and water [28–31]. The RKSA-Infochem + electrolyte equation of state is less known from the literature, but it has been extensively used by the oil and gas industry.

Both EoS have been used with default Multiflash™ 4.4 interaction parameters at all times. No interaction parameters have been fitted to the experimental data measured in this work.

4. Results and discussion

Although measurements were previously carried by us and others in similar apparatuses and the methodology shown to be adequate to accurately measure gas–liquid equilibria in a wide range of pressures, temperatures and fluids, such as alkanes and ionic liquids and their aqueous solutions [10–13,15–17,32], the carbon dioxide solubility in water and aqueous solutions of salts can introduce an additional complexity to the experimental determination, like salt precipitation and/or equipment corrosion. Thus, $H_2O + CO_2$ and $H_2O + CO_2 + NaCl$ systems were investigated to

Table 2
Bubble point data of the system $CO_2 + H_2O + NaCl$.

x_{CO2}	T/K	p/MPa	x_{CO2}	T/K	p/MPa	x_{CO2}	T/K	p/MPa
m_{NaCl} = 0.25 mol kg^{-1}								
0.007	293.37	1.02	0.012	293.42	2.01	0.017	293.30	2.94
	313.28	1.81		313.07	3.70		313.21	5.51
	333.31	2.73		333.06	5.56		333.03	8.81
	353.22	3.51		352.95	7.34		352.91	11.39
m_{NaCl} = 0.50 mol kg^{-1}								
0.007	293.08	1.21	0.012	293.38	2.17	0.017	293.17	3.34
	313.18	2.14		313.20	3.91		313.36	6.40
	333.24	3.13		333.12	5.98		333.18	9.75
	353.12	3.96		353.05	7.78		353.18	12.53
m_{NaCl} = 1.0 mol kg^{-1}								
0.007	293.20	1.35	0.013	293.33	2.48	0.017	293.28	3.95
	313.10	2.40		313.35	4.42		313.30	7.62
	332.92	3.54		333.17	6.75		332.88	12.25
	353.23	4.72		352.97	8.51			
m_{NaCl} = 2.0 mol kg^{-1}								
0.007	293.34	1.78	0.013	293.17	3.76	0.018	293.27	10.59
	313.19	3.00		313.19	6.75			
	333.19	4.41		333.03	10.64			
	353.14	5.72		353.16	14.29			

Standard uncertainties u are $u(T)$ = 0.15 K, $u(x)$ = 0.0002, $u(p)$ = 0.004 MPa and $u(m)$ = 0.005 mol kg^{-1}.

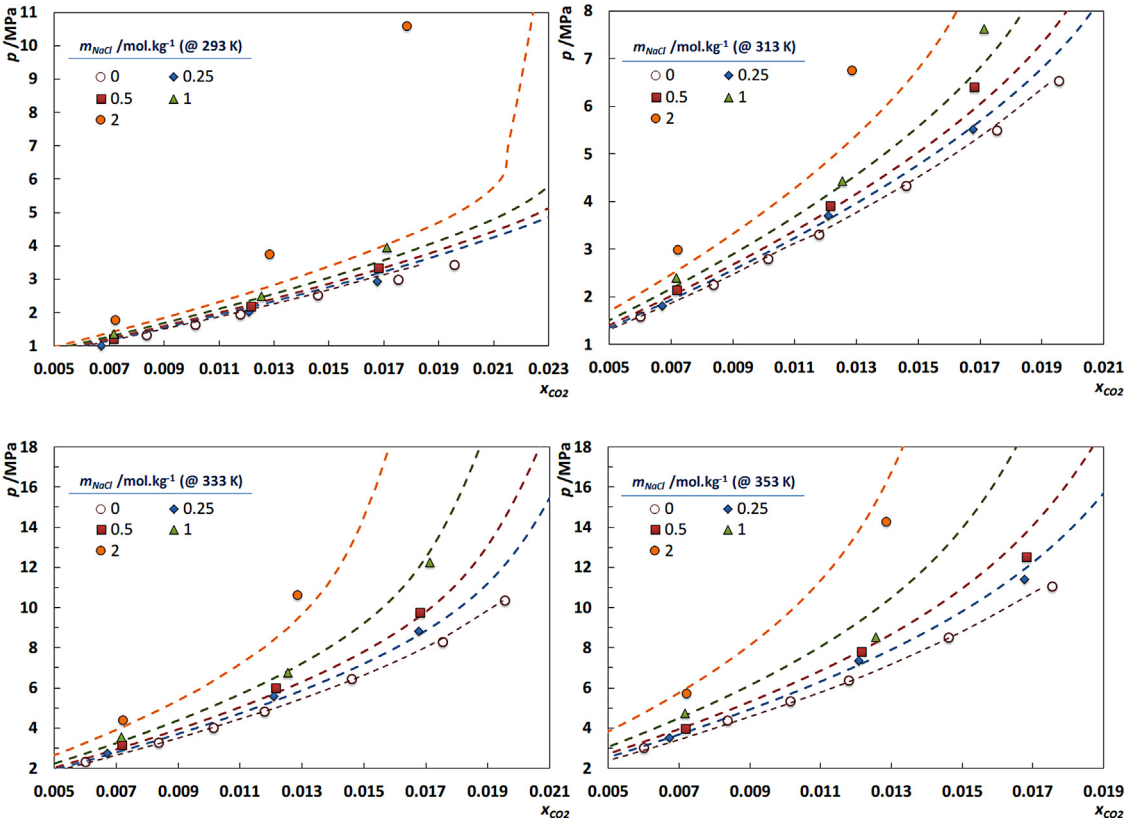

Fig. 3. Pressure–composition diagrams of the system $CO_2 + H_2O + NaCl$. The dashed lines represent the RKSA-Infochem EoS estimates.

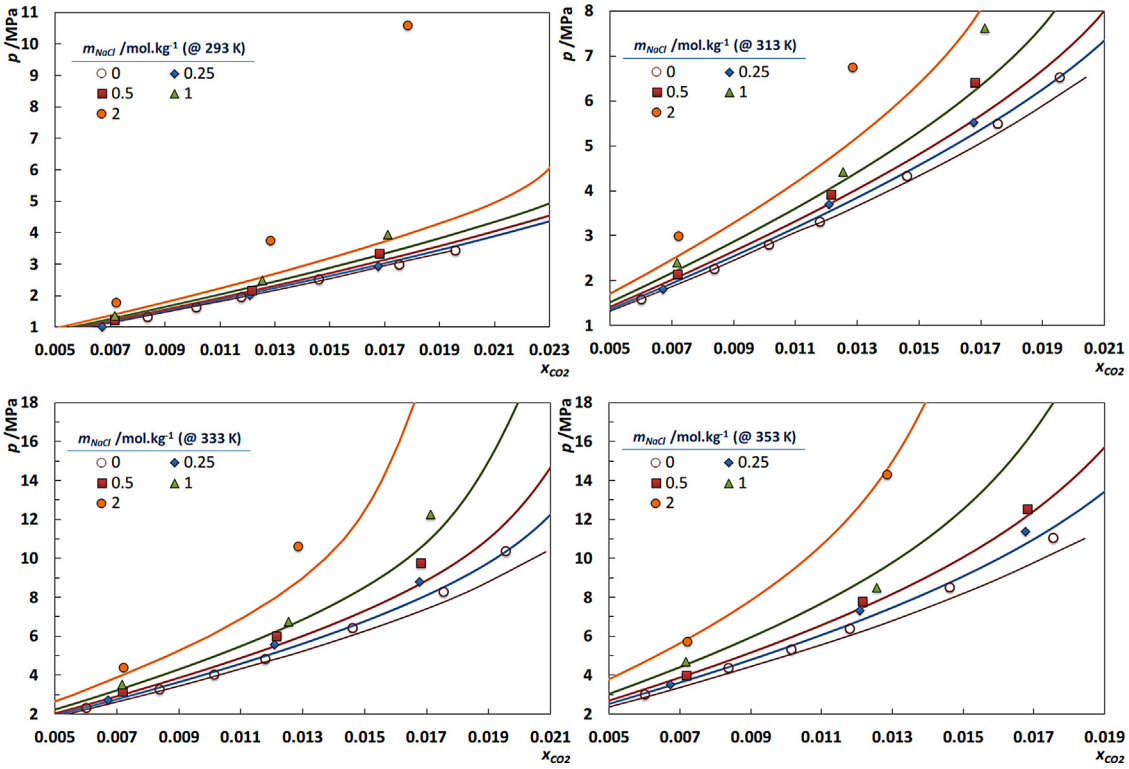

Fig. 4. Pressure–composition diagrams of the system $CO_2 + H_2O + NaCl$. The solid lines represent the CPA EoS estimates.

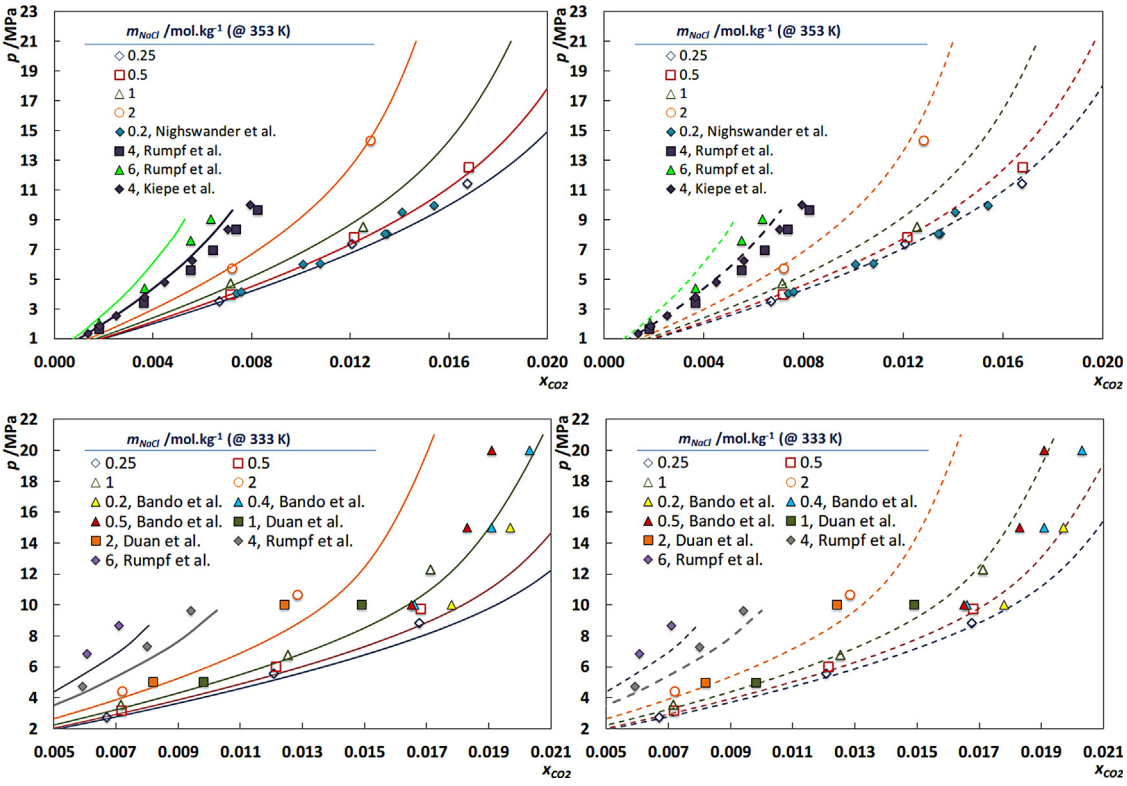

Fig. 5. Pressure–composition diagrams of the system $CO_2 + H_2O + NaCl$. The solid and dashed lines represent, respectively, the CPA EoS and RKSA-Infochem with electrolyte term estimates. Solid and empty symbols represent literature [39,41,46,47,60] and experimental data, respectively.

validate both the equipment and methodology through comparison against available literature data.

4.1. Solubility of CO_2 in water

Carbon dioxide solubility in water was measured in the temperature range (283–363) K and pressures up to 13 MPa, as reported in Table 1 and depicted in Fig. 1. Gas–liquid equilibrium data for the $CO_2 + H_2O$ binary system is widely available in literature covering a large range of pressures, temperatures and compositions [33–50].

The equilibrium data obtained is in good agreement with literature data within the temperature, pressure and carbon dioxide compositions investigated, as depicted in Fig. 2. Literature vapor–liquid equilibrium data was collected from sources dating from 1939 to 2013 and plotted against our experimental data, as depicted in Fig. 2a, and the pressure deviations

$$\Delta p = \frac{\Sigma_1^n |p_{exp} - p_{lit}|}{n} \quad (2)$$

were calculated, showing an absolute average deviation of 0.11 MPa (%AAD of 8.46%) for over 21 sources and 300 data points, as depicted in Fig. 2b. Moreover, the experimental data are in close agreement with the data of Wiebe and Gaddy [34], Valtz et al. [43], Campos et al. [44], Dalmolin et al. [45] and Rumpf et al. [41] with absolute average pressure deviations of 0.09, 0.04, 0.02, 0.02 and 0.06 MPa, respectively. The highest deviations were found for the data of Li et al. [50], Briones et al. [42], Nighswander et al. [46], Kiepe et al. [47] (at 313 K), Teng and Yamasaki [49] and Yan et al. [40] with absolute average pressure deviations of 0.99, 0.86, 0.20, 0.12, 0.72 and 0.54 MPa, respectively. Despite the higher deviations found with the later sets of data, the equilibrium pressures obtained at low carbon dioxide mole fractions are in close agreement among all the authors, being the deviations noticeable for CO_2 compositions higher than 0.015 and for the highest temperatures investigated. Furthermore, the data by Kiepe et al. [47] for temperatures higher than 313 K present an inconsistent behavior, with their 353 K and 373 K isotherms crossing through ours 353 K and 333 K, and 373 K and 353 K isotherms, respectively. Overall, the small deviations obtained validate both the above described high pressure equilibrium cell and methodology adopted, showing them to be adequate to measure these type of systems.

As depicted in Fig. 1a, the CPA-Infochem + electrolyte EoS is able to estimate the experimental data over all the gas composition and temperature range with a carbon dioxide mole fraction solubility uncertainty of 1.5×10^{-3} and a pressure absolute average deviation (%AAD) of 5.7%. The model slightly under-estimates the CO_2 equilibrium pressures for temperatures higher than 313 K. The RKSA-Infochem + electrolyte EoS estimates are in good agreement with the experimental data over all the temperature and carbon dioxide compositions range, with a carbon dioxide mole fraction

Table 3
Henry's constants, $H_{CO_2,L}$/MPa, for the studied systems.

$CO_2 + H_2O + NaCl$					
	m_{NaCl}/mol kg^{-1}				
T/K	0	0.25	0.5	1	2
283.15	129.20				
293.15	158.69	169.76	174.32	182.67	197.13
303.15	210.80				
313.15	242.66	263.53	273.12	291.19	324.55
323.15	301.62				
333.15	346.76	373.54	391.28	425.77	493.33
343.15	403.25				
353.15	459.81	501.60	531.88	592.48	717.97
363.15	512.68				

Standard uncertainties u are $u(T) = 0.15$ K and $u(m) = 0.005$ mol kg^{-1}.

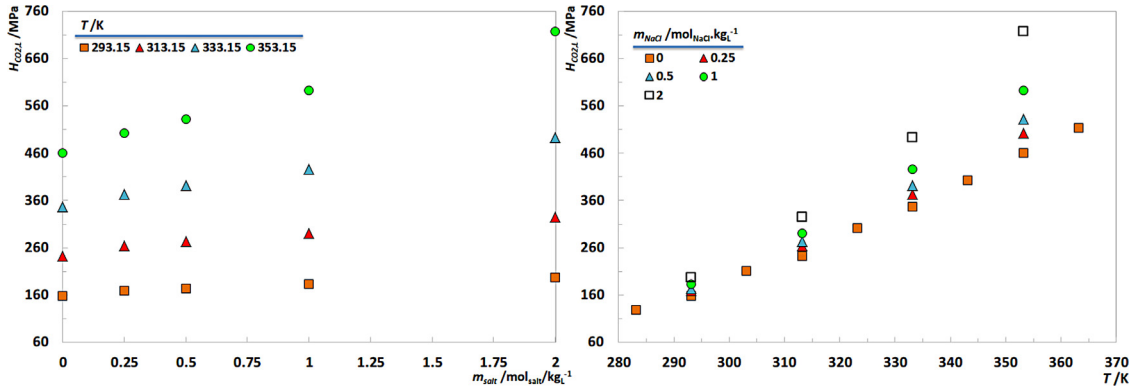

Fig. 6. Henry's constants of the studied system.

uncertainty of 2.2×10^{-3} and a pressure %AAD of 7.1%, as depicted in Fig. 1b.

4.2. Solubility of CO_2 in aqueous solutions of NaCl

Carbon dioxide solubility in aqueous solutions of NaCl was measured at (293, 313, 333 and 353) K, pressures up to 14 MPa and for NaCl molalities of 0.25, 0.5, 1 and 2, as reported in Table 2 and as depicted in Figs. 3 and 4.

As well established, it is observed that NaCl promotes a *salting out* effect on the carbon dioxide solubility in water decreasing its solubility when compared with pure water. The *salting out* effect depends on the ions charge and radius, salt concentration, temperature and the static dielectric constant of the solvent. The interactions of the ions and the solute are partially shielded by the hydration shell forming which, in turn, influences the solvation energy and ultimately the gas solubility [54–58].

Gas solubility data for the $CO_2 + H_2O + NaCl$ ternary system is available in the literature [40,41,46,47,51,59–61] but not as extensively as for the $CO_2 + H_2O$ binary. Furthermore, the available data present important discrepancies not only between different authors but also within the same data source. Yan et al. [40] presents equilibrium pressures for the 413 K isotherms, for both salt molalities reported, that cross the lower isotherms for carbon dioxide mole fractions higher than 0.015. Bando et al. [60] reports equilibrium pressures higher than those reported by the other authors, as depicted in Fig. 5. Nonetheless, for the data at the same salt molalities and temperatures investigated here, absolute average pressure deviations of 0.46 MPa and 0.16 MPa were obtained against the data of Kiepe et al. [47] and Duan and Sun [39], respectively. Although the data of Duan et al. [39,62] is the result of a model, based on the Duan et al. [63] EoS and the theory of Pitzer [64], fitted against experimental data with an experimental uncertainty of 7%, the experimental data here measured is in very good agreement, with absolute average pressure deviations of 0.36 MPa, with the data from all these sources.

As depicted in Figs. 3 and 5, the RKSA-Infochem + electrolyte EoS is able to estimate the experimental data over all the gas compositions and temperature range, with a carbon dioxide mole fraction uncertainty of 7.6×10^{-4} and an absolute average deviation of 9.4%. Although, the EoS fails to estimate the equilibrium pressures for the 2 mol kg^{-1} salt molality at 293 K, Fig. 3, it only slightly under-estimates the equilibrium pressures for temperatures lower than 333 K. For higher temperatures the RKSA-Infochem + electrolyte EoS slightly over-estimates the equilibrium pressure over all the salt molalities investigated. Even though the CPA-Infochem + electrolyte EoS presents similar trends as those observed for the RKSA-Infochem + electrolyte EoS, as depicted in Figs. 4 and 5, it presents somewhat higher carbon dioxide mole fraction uncertainties, 1.2×10^{-3}, which corresponds to an absolute average deviation of 12%.

Overall and despite the deviations observed, both equations of state are able to estimate the $CO_2 + H_2O$ and $CO_2 + H_2O + NaCl$ systems with low carbon dioxide mole fraction solubility uncertainties. The capacity of these EoS to estimate both the binary and the ternary systems stands out as very good if one takes into considerations the scale of the CO_2 compositions, its order of magnitude and its strong effect on the equilibrium pressure.

4.3. Henry's constant

The Henry's law relates the amount of a given gas dissolved in a liquid, at a constant temperature, to the fugacity of that gas in equilibrium with that liquid and can be described as

$$H_{CO_2,L}(T,p) = \lim_{x_{CO2}\to 0} \frac{f^L_{CO_2}}{x_{CO2}} \tag{3}$$

where $H_{CO_2,L}(T,p)$ is the Henry's constant, x_{CO2} is the mole fraction of CO_2 dissolved in the liquid and $f^L_{CO_2}$ is the fugacity of CO_2 in the liquid phase (L). As shown, Eq. (3) is only rigorously valid in the diluted region limit. The Henry's constants were estimated by fitting the RKSA-Infochem + electrolyte to the experimental data and calculating the slope as the solubility approaches zero. Although this procedure introduces some uncertainty on the estimated Henry's constants, the results obtained allow a discussion on the solvation of the CO_2 in the solvents investigated.

The Henry's constant for the CO_2 in water and NaCl solutions are reported in Table 3 and depicted in Fig. 6. As shown, the Henry's constants express the *salting out* effect of the salt on the carbon dioxide solubility in water, with the Henry's constant increasing with the temperature and salt molality. Furthermore, the temperature impact on the gas solubility is more pronounced, increases, with the salt molality increase.

5. Conclusions

A new high pressure cell was developed and validated to measure the high pressure phase behavior of gas + water and gas + aqueous salt solutions. Two systems, the $H_2O + CO_2$ and $H_2O + CO_2 + NaCl$, were investigated at temperatures up to 363 K and pressures up to 13 MPa and both the equipment and methodology validated through comparison against literature data. As commonly observed in literature the NaCl promotes a *salting out* effect on the carbon dioxide solubility in water, decreasing its solubility in water as the salt concentration increase.

Electrolyte versions of the cubic-plus-association and the RKSA-Infochem equations of state were used to estimate the

$H_2O + CO_2$ and $H_2O + CO_2$ + NaCl phase behavior. Both EoS provide a good representation of the experimental data, with the RKSA-Infochem + electrolyte EoS slightly out-performing the CPA-Infochem + electrolyte EoS.

Acknowledgements

The authors acknowledge FEDER funds through the COMPETE operational program, Fundação para a Ciência e Tecnologia - FCT through the projects PTDC/QUI-QUI/121520/2010 and PEst-C/CTM/LA0011/2013 and post-doctoral Grant SFRH/BPD/82264/2011 of P.J. Carvalho.

References

[1] J. Gibbins, Science for Environment Policy. European Commission DG Environment News Alert Service, 3 (2008) (special issue).
[2] J. Yu, M. Khalil, N. Liu, R. Lee, Fuel 126 (2014) 104–108.
[3] A. Ettehad, Greenh. Gases Sci. Technol. 4 (2014) 66–80.
[4] S.H. Talebian, R. Masoudi, I.M. Tan, P.L.J. Zitha, J. Petrol. Sci. Eng. 120 (2014) 202–215.
[5] J.R. Christensen, E.H. Stenby, A. Skauge, SPE Reserv. Eval. Eng. 4 (2013) 97–106.
[6] S. Vitu, J.N. Jaubert, J. Pauly, J.L. Daridon, D. Barth, J. Supercrit. Fluids 44 (2008) 155–163.
[7] J. Pauly, J. Coutinho, J.L. Daridon, Fluid Phase Equilib. 255 (2007) 193–199.
[8] A.M.A. Dias, H. Carrier, J.L. Daridon, J.C. Pàmies, L.F. Vega, J.A.P. Coutinho, I.M. Marrucho, Ind. Eng. Chem. Res. 45 (2006) 2341–2350.
[9] S.P.M. Ventura, J. Pauly, J.L. Daridon, I.M. Marrucho, A.M.A. Dias, J.A.P. Coutinho, J. Chem. Eng. Data 52 (2007) 1100–1102.
[10] S. Mattedi, P.J. Carvalho, J.A.P. Coutinho, V.H. Alvarez, M. Iglesias, J. Supercrit. Fluids 56 (2011) 224–230.
[11] P.J. Carvalho, V.H. Alvarez, B. Schröder, A.M. Gil, I.M. Marrucho, M. Aznar, L.M.N. B.F. Santos, J.A.P. Coutinho, J. Phys. Chem. B 113 (2009) 6803–6812.
[12] P.J. Carvalho, V.H. Álvarez, I.M. Marrucho, M. Aznar, J.A.P. Coutinho, J. Supercrit. Fluids 50 (2009) 105–111.
[13] P.J. Carvalho, J.A.P. Coutinho, Energy Environ. Sci. 4 (2011) 4614–4619.
[14] L.M.C. Pereira, M.B. Oliveira, A.M.A. Dias, F. Llovell, L.F. Vega, P.J. Carvalho, J.A.P. Coutinho, Int. J. Greenh. Gas Control 19 (2013) 299–309.
[15] P.J. Carvalho, V.H. Álvarez, J.J.B. Machado, J. Pauly, J.-L. Daridon, I.M. Marrucho, M. Aznar, J.A.P. Coutinho, J. Supercrit. Fluids 48 (2009) 99–107.
[16] P.J. Carvalho, J.A.P. Coutinho, J. Phys. Chem. Lett. 1 (2010) 774–780.
[17] S.P.M. Ventura, J. Pauly, J.L. Daridon, J.A.L. da Silva, I.M. Marrucho, A.M.A. Dias, J. A.P. Coutinho, J. Chem. Thermodyn. 40 (2008) 1187–1192.
[18] G.M. Kontogeorgis, M.L. Michelsen, G.K. Folas, S. Derawi, N. von Solms, E.H. Stenby, Ind. Eng. Chem. Res. 45 (2006) 4869–4878.
[19] G.M. Kontogeorgis, M.L. Michelsen, G.K. Folas, S. Derawi, N. von Solms, E.H. Stenby, Ind. Eng. Chem. Res. 45 (2006) 4855–4868.
[20] N. Pedrosa, R. Szczepanski, X. Zhang, Fluid Phase Equilib. 359 (2013) 24–37.
[21] M.B. Oliveira, J.A.P. Coutinho, A.J. Queimada, Fluid Phase Equilib. 258 (2007) 58–66.
[22] I. Tsivintzelis, G.M. Kontogeorgis, M.L. Michelsen, E.H. Stenby, Fluid Phase Equilib. 306 (2011) 38–56.
[23] S.P. Tan, H. Adidharma, M. Radosz, Ind. Eng. Chem. Res. 47 (2008) 8063–8082.
[24] G.M. Kontogeorgis, G.K. Folas, Thermodynamic Models for Industrial Applications, John Wiley & Sons, Ltd., Chichester, UK, 2010.
[25] M.B. Oliveira, F.R. Varanda, I.M. Marrucho, A.J. Queimada, J.A.P. Coutinho, Ind. Eng. Chem. Res. 47 (2008) 4278–4285.
[26] M.B. Oliveira, S.I. Miguel, A.J. Queimada, J.A.P. Coutinho, Ind. Eng. Chem. Res. 49 (2010) 3452–3458.
[27] M.B. Oliveira, A.J. Queimada, J.A.P. Coutinho, J. Supercrit. Fluids 52 (2010) 241–248.
[28] M.B. Oliveira, V. Ribeiro, A.J. Queimada, J.A.P. Coutinho, Ind. Eng. Chem. Res. 50 (2011) 2348–2358.
[29] M.B. Oliveira, A.J. Queimada, J.A.P. Coutinho, Ind. Eng. Chem. Res. 49 (2010) 1419–1427.
[30] L.A. Follegatti-Romero, M. Lanza, F.R.M. Batista, E.A.C. Batista, M.B. Oliveira, J.A. P. Coutinho, A.J.A. Meirelles, Ind. Eng. Chem. Res. 49 (2010) 12613–12619.
[31] M.B. Oliveira, A.J. Queimada, G.M. Kontogeorgis, J.A.P. Coutinho, J. Supercrit. Fluids 55 (2011) 876–892.
[32] P.J. Carvalho, A.R. Ferreira, M.B. Oliveira, M. Besnard, M.I. Cabaço, J.A.P. Coutinho, J. Chem. Eng. Data 56 (2011) 2786–2792.
[33] A. Bamberger, G. Sieder, G. Maurer, J. Supercrit. Fluids 17 (2000) 97–110.
[34] R. Wiebe, V.L. Gaddy, J. Am. Chem. Soc. 62 (1940) 815–817.
[35] R. Wiebe, V.L. Gaddy, J. Am. Chem. Soc. 61 (1939) 315–318.
[36] R. Wiebe, Chem. Rev. 29 (1941) 475–481.
[37] J.J. Carroll, J.D. Slupsky, A.E. Mather, J. Phys. Chem. Ref. Data 20 (1991) 1201–1209.
[38] H. Teng, A. Yamasaki, M.-K. Chun, H. Lee, J. Chem. Thermodyn. 29 (1997) 1301–1310.
[39] Z. Duan, R. Sun, Chem. Geol. 193 (2003) 257–271.
[40] W. Yan, S. Huang, E.H. Stenby, Int. J. Greenh. Gas Control 5 (2011) 1460–1477.
[41] B. Rumpf, H. Nicolaisen, C. Öcal, G. Maurer, J. Solut. Chem. 23 (1994) 431–448.
[42] J. Briones, J. Mullins, M. Thies, B. Kim, Fluid Phase Equilib. 36 (1987) 235–246.
[43] A. Valtz, A. Chapoy, C. Coquelet, P. Paricaud, D. Richon, Fluid Phase Equilib. 226 (2004) 333–344.
[44] C.E.P.S. Campos, H.G.D. Villardi, F.L.P. Pessoa, A.M.C. Uller, J. Chem. Eng. Data 54 (2009) 2881–2886.
[45] I. Dalmolin, E. Skovroinski, A. Biasi, M.L. Corazza, C. Dariva, J.V. Oliveira, Fluid Phase Equilib. 245 (2006) 193–200.
[46] J.A. Nighswander, N. Kalogerakis, A.K. Mehrotra, J. Chem. Eng. Data 34 (1989) 355–360.
[47] J. Kiepe, S. Horstmann, K. Fischer, J. Gmehling, Ind. Eng. Chem. Res. 41 (2002) 4393–4398.
[48] G. Houghton, A.M. McLean, P.D. Ritchie, Chem. Eng. Sci. 6 (1957) 132–137.
[49] H. Teng, A. Yamasaki, Chem. Eng. Commun. 189 (2002) 1485–1497.
[50] Z. Li, M. Dong, S. Li, L. Dai, J. Chem. Eng. Data 49 (2004) 1026–1031.
[51] D. Koschel, J.-Y. Coxam, L. Rodier, V. Majer, Fluid Phase Equilib. 247 (2006) 107–120.
[52] S.-X. Hou, G.C. Maitland, J.P.M. Trusler, J. Supercrit. Fluids 73 (2013) 87–96.
[53] A. Chapoy, A.H. Mohammadi, A. Chareton, B. Tohidi, D. Richon, Ind. Eng. Chem. Res. 43 (2004) 1794–1802.
[54] M. Görgényi, J. Dewulf, H. Van Langenhove, K. Héberger, Chemosphere 65 (2006) 802–810.
[55] A. Hasseine, A.-H. Meniai, M. Korichi, Desalination 242 (2009) 264–276.
[56] M.J. Hey, D.P. Jackson, H. Yan, Polymer 46 (2005) 2567–2572.
[57] F.J. Millero, F. Huang, A.L. Laferiere, Mar. Chem. 78 (2002) 217–230.
[58] M. Boström, B.W. Ninham, J. Phys. Chem. B 108 (2004) 12593–12595.
[59] Y. Liu, M. Hou, G. Yang, B. Han, J. Supercrit. Fluids 56 (2011) 125–129.
[60] S. Bando, F. Takemura, M. Nishio, E. Hihara, M. Akai, J. Chem. Eng. Data 48 (2003) 576–579.
[61] S.-X. Hou, G.C. Maitland, J.P.M. Trusler, J. Supercrit. Fluids 78 (2013) 78–88.
[62] Z. Duan, R. Sun, C. Zhu, I.-M. Chou, Mar. Chem. 98 (2006) 131–139.
[63] Z. Duan, N. Møller, J.H. Weare, Geochim. Cosmochim. Acta 56 (1992) 2605–2617.
[64] K.S. Pitzer, J. Phys. Chem. 77 (1973) 268–277.